Proceedings of the 2005 Winter Simulation Conference
M. E. Kuhl, N. M. Steiger, F. B. Armstrong, and J. A. Joines, eds.

SIMULATION BASED PERFORMANCE MODELING FOR A WARFIGHTER IN THE LOOP MINEFIELD DETECTION SYSTEM

Abhilash Rajagopal
Sanjeev Agarwal

Electrical and Computer Engineering Department
University of Missouri - Rolla
Rolla, MO 65409, U.S.A.

Sreeram Ramakrishnan

Engineering Management and Systems Engineering
University of Missouri - Rolla
Rolla, MO 65409, U.S.A.

ABSTRACT

There has been significant recent interest in airborne reconnaissance for target detection using high resolution airborne images collected from an Unmanned Aerial Vehicle (UAV). Even if Automatic Target Recognition (ATR) algorithms are able to produce satisfactory results in terms of probability of detection for certain false alarm rate, there is a need for a Warfighter-in-the-Loop (WIL) to reduce false alarms further and verify and validate detections to attain the operational performance requirements. We develop a simulation model to assess effectiveness of the warfighter in decision loop for airborne minefield detection. The warfighter effectiveness is measured in terms of average waiting-time, number of minefield segments in queue, and the expected false alarms, and missed detection. Various parameters which potentially affect the warfighter performance were identified with the help of prior studies with human operator in laboratory settings. Simulation trials were conducted to evaluate the dependence of these parameters on warfighter performance.

1 INTRODUCTION

1.1 Airborne Minefield Detection

The process of determining the existence of mines in a particular region is typically a manual process involving handheld devices. Clearly, such an approach puts the human at elevated risk. The personnel are exposed to enemy forces and also to undetected mines. On the other hand, the human intelligence required to determine the presence or absence of mines in an area of interest, cannot be completely automated. In order to mitigate these risks, mine detection process is transforming into a semi-automated stand-off detection system such as airborne minefield detection with warfighter in the loop.

Airborne detection has the advantage of being safer and potentially more efficient than traditional minefield detection methods. In airborne detection, manned, and unmanned aircraft with a wide variety of sensors attempt to identify minefields. Airborne detection has many advantages like it is safer than requiring soldiers to physically locate and identify minefields using techniques such as handheld mine detectors. Furthermore, the use of unmanned drones can further reduce the risk by eliminating the need for pilots to fly over hostile territory. Sensors employing different modalities such as near infra-red (NIR) and mid-wave infra-red (MWIR) can be used to identify mines. Individual mine detectors are used to make decision on presence and extent of the minefields. Airborne detection can also provide battlefield commanders with enough advanced warning about minefield locations that they can use to make decision about how they want to handle the situation.

1.2 Minefield Detection Algorithms

Even though airborne detection seems to be a safer method for detecting minefields, its efficiency depends on different algorithms which will analyze the image data to detect individual mines and minefields. There are several algorithms which determine presence of mines and minefields using visual features of the airborne image obtained from the UAV (Reed and Yu 1990, Earp, Elkins, and Conrath 1995). Factors such as the thermal signature of the mine, its shape, pattern, shadow are employed by algorithms to determine whether a given feature is a mine. Mine detection methods often use an anomaly detector such as RX detector (Reed and Yu 1990, Homes, Schwartz, Seldin, Wright, and Witter 1995) to detect possible mine locations. Mine detection block may also use a false alarm mitigation process to reduce the false alarm rate (Sriram, Agarwal and Mitchell 2002). Even though algorithms are improving, fully automatic target recognition process still fails to satisfy the operational requirements of minefield detection. This necessitates human interaction for verification and decision making.

1.3 Role of Warfighter in Minefield Detection

The warfighter plays an extremely important role in airborne detection. He/she must make rapid decisions about the existence of minefields sometimes under highly stressful conditions. However, we have relatively little understanding of how warfighters perform in minefield detection, what techniques they use to identify the presence or absence of a minefield, and what interface features best support their detection capabilities. Several tests were conducted using a MATLAB-based graphical user interface for mine level as well as for minefield level detection (Reddy, Agarwal, Hall, Brown, and Woodard 2005 and Agarwal, Reddy, Hall, Brown, and Woodard 2005) to study some of these factors.

The experiment used airborne data collected at two different test sites of the US Army. Both military and non-military personnel were used in the experiments. The purpose of these experiments was to analyze a warfighter's performance when a set of images are presented at a constant rate. In real time situations, the warfighter might have to handle images from not just a single UAV, but from multiple streams of data from different fields, and may in fact be multi-tasking. Moreover, the mental stress of the warfighter should also be considered. This paper discusses some of the observations from the above mentioned experiments and discusses a simulation model that is used to analyze the system performance (here, the system is defined as the ATR and the human personnel combined) under varying conditions such as arrival rates and processing times. The results obtained from the simulation analysis can be used for specifying the performance metrics for the individual components in the minefield detection system.

2 PROBLEM STATEMENT AND RESEARCH OBJECTIVES

The overall objective of this paper is to identify performance drivers for a warfighter in a semi-automated minefield detection system, where the warfighter acts as the second decision maker to an automated minefield detection algorithm(s).

2.1 Objectives

The motivating problem for this research is the need to characterize system performance in scenarios with data streams from multiple UAVs, fed to a single warfighter-in-the-loop. In order to accomplish that task, it is critical to understand the system behavior when only a single stream is considered. This paper addresses this modeling need for the domain, and will enable developing analytical models for single data stream and multiple data stream scenarios. Such a modeling effort will help in specifying and characterizing the system components appropriately.

2.2 Simulation Framework

The factors such as the arrival rates, number of streams of data, modeling of processing time, and the false-positive, and false-negative rates associated with the ATR (automated algorithm), and the warfighter are discussed in the context of performance characterization. The simulation model will help identify the best operating conditions for the semi-automated system, with specific focus on the average waiting time for the data segments in the queues associated with the warfighter.

3 PERFORMANCE MODELING

The basic model with a single stream of data is given in Figure 1. The raw image data was collected from airborne sensor flying through a particular area. In this simulation, the following data were used: flight speed is 70 knots and with a frame rate of approximately 8 Hz. The swath width for the sensor is about 15 meters. In this model, the raw imagery of registered minefield size segment typically representing approximately 60m x 120m on ground is processed by ATR for mine level detections. ATR uses algorithms such as RX (Reed and Yu 1990), and Radial Anomaly Detector (Menon, Agarwal, Ganju, and Swonger 2004). Individual mine targets in the minefield size segment are further analyzed for patterns of potential minefield using minefield algorithms (Earp, Elkins, and Conrath 1995). Both ATRs are considered as a single component in the current simulation. The required probability of detection of ATR at the minefield level is 95% with a false alarm rate of less than 0.5FA/km^2 The minefield segments flagged by the ATR are passed to the warfighter for final verification and decision making. The probability of detection at the WIL level is expected to be 95% with a false alarm rate of less than 0.1 FA/km^2.

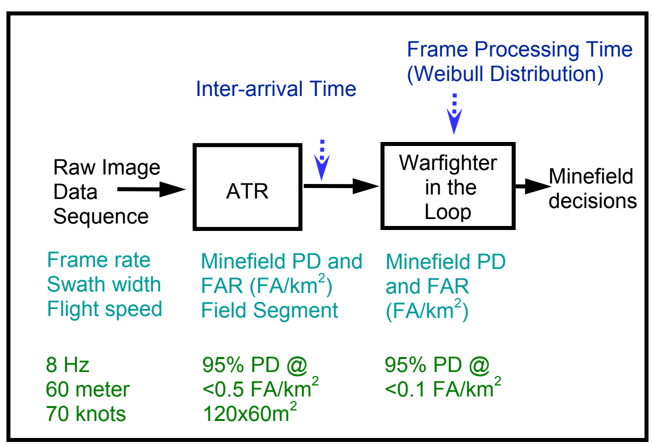

Figure 1: Mine Detection Model for Data from a Single UAV

Time taken by the subjects to make decision was considered at the WIL stage. The false-positive (flagging a segment known to be mine-free as a minefield), and false-negative rates of humans were also studied. In this study, mental stress and other physical conditions such as climate were not controlled or modeled.

3.1 Automatic Target Recognition System

The image segments are passed into the ATR in the order in which they are received from the UAV at a rate of approximately 1/3 Hz. For our analysis, we have a ground-truth database which has the information whether the segment is a minefield or a non-minefield. Several algorithms have been developed to detect mines based on their image features. Different characteristics of the mines, such as circularity, and gray moments were used to detect anomalies. These anomalies detected by ATR do not necessarily have to be mines. It could be rocks or bushes having similar signatures. These are mine-level false alarms. The ATR's decision, whether the analyzed segment is a minefield or not, depends on the concentration and distribution of anomalies in the segment. If the threshold level is reached, the ATR flags it as a minefield segment. Non-mine targets flagged as mines can sometimes form spatial distribution pattern that is minefield like. The non-minefield segments that are flagged by the ATR are called minefield false alarms. Only a certain small fraction of the total non-minefield segments are passed by ATR as false alarms. Only segments which are flagged as minefields by the ATR are passed on to the warfighter for further visual analysis.

3.2 Warfighter Performance

Some preliminary analysis was done to evaluate warfighter's performance for minefield detection using airborne imagery. The experiments and results are described in greater detail in (Reddy, Agarwal, Hall, Brown, and Woodard 2005) and (Agarwal, Reddy, Hall, Brown, and Woodard 2005). A set of 26 runs of images were selected which covered a total area of 1.34 km^2. ATR triggered 0.4 km^2 as having high probability of containing minefields. In order to facilitate the experiment, minefield segments were chosen to form an even distribution of data from mine/no-mine, time of day, and two different backgrounds. The purpose of this evaluation was to characterize the human processing time in minefield detection. The other factors which are considered in this paper are the probability of detection and false alarm rate of the warfighter. Some factors such as the mental and physical situation of the WIL in an actual war, the other duty constraints are quite significant but are not considered here.

3.3 Warfighter's Time Response Characteristic

For the tests conducted on 10 subjects, the analysis was performed by splitting the data into minefield segments and non-minefield segments. The time taken to select the corresponding segment was recorded for each user. Distribution of time taken by the users for segments with mines and segments without mines was evaluated. Figure 2 and Figure 3 shows the distribution for segments with mines and segment without mines respectively. These results show that users typically need more time to analyze segments which have actual mines in it than non-mine segments.

The scale, shape, and offset parameters of the Weibull distributions were used to model the processing time in the simulation model. A random variable X has a Weibull distribution if there are values of parameters such as, shape: c(>0), scale: α(>0), and time delay: ξ_0 such that:

$$Y = \left(\frac{X - \xi_0}{\alpha} \right)^c, \; y > 0 \tag{1}$$

The probability density function of the random variable X is given as:

$$p_X(x) = \frac{c}{\alpha^c} \left(x - \xi_0 \right) e^{-\left(\frac{x - \xi_0}{\alpha} \right)^c}, \; x > \xi_0 \tag{2}$$

The observed values and the fitted distributions are shown in Figure 2 (for segments with mines; scale = 27.6378, shape = 1.3838, time delay = 5) and Figure 3 (for no mine segments; scale = 16.2908, shape = 0.9916, time delay = 3). These observed and modeled time distribution in Figure 2 and 3 suggest that a Weibull distribution can be used to model the time-response characteristic of the warfighter.

4 SIMULATION EXPERIMENTS

4.1 Simulation Framework and Controllable Parameters

The problem can be well understood by the simulation framework given in Figure 4. Figure 5 shows the flagging of the frames which is explained later. The major components: ATR processing block, WIL processing block, and the modeled factors associated with them are shown in the figure, and are discussed in the following subsections.

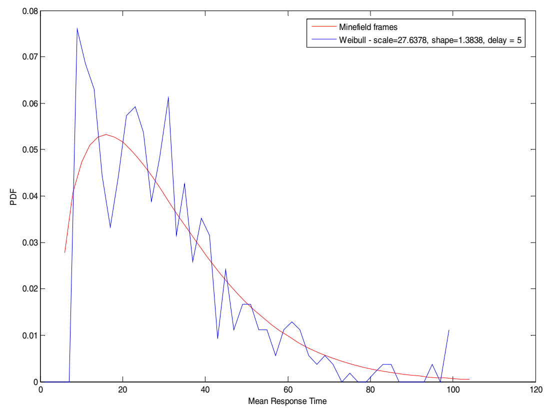

Figure 2: Processing Time for Segments With Mines

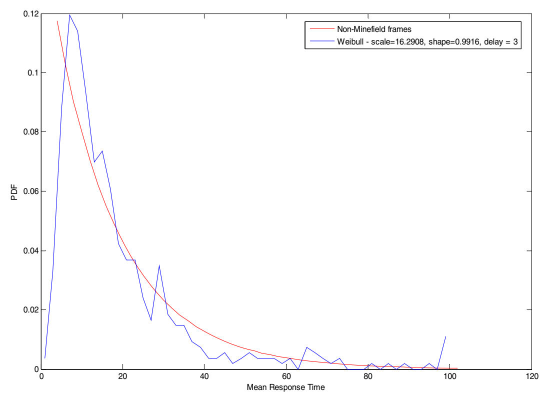

Figure 3: Processing Time for Segments Without Mines

4.1.1 Input Stage

There are three controllable parameters in the input stage: the frame rate, proportion of minefield/no-minefield data, and number of streams of UAV data. Image segments of given size are acquired at some constant rate and is fed at the input stage. For the current simulation, a constant frame rate of 1 segment per 3 seconds is assumed. These image segments are flagged as follows:

- Y : For minefield
- N : For non-minefield

The image segment data has associated tags (Y/N) in each frame which shows whether it is a minefield segment or a non-minefield segment. These flagged images are passed into the ATR for detection. The ATR does not have any prior information regarding the presence or absence of a minefield in any given segment.

The proportion of minefield/non-minefield is also an important controllable factor that can be varied for analysis. The percentage of non-minefield segments would typically be much greater than the minefield segments. The last controllable factor is the number of streams that can be given as input. The warfighter can only handle a certain number of segments since he/she takes time to evaluate each segment. So analysis can be done to determine the optimum number of streams a warfighter can handle. This issue is considered beyond the scope of this paper, but will be studied in the future as a continuation of the work discussed here.

4.1.2 ATR Stage

There are three controllable parameters in the ATR stage. They are the ATR processing time, ATR false alarm rate, and the ATR probability of detection. The ATR takes a definite processing time to analyze the segments. We expect a near real time automatic target processing and thus the average time for ATR processing should be less than the frame arrival interval. The probability of detection and the false alarm rate of the ATR represents the efficiency of the algorithm implemented for correctly detecting minefields and wrongly detecting non-minefields.

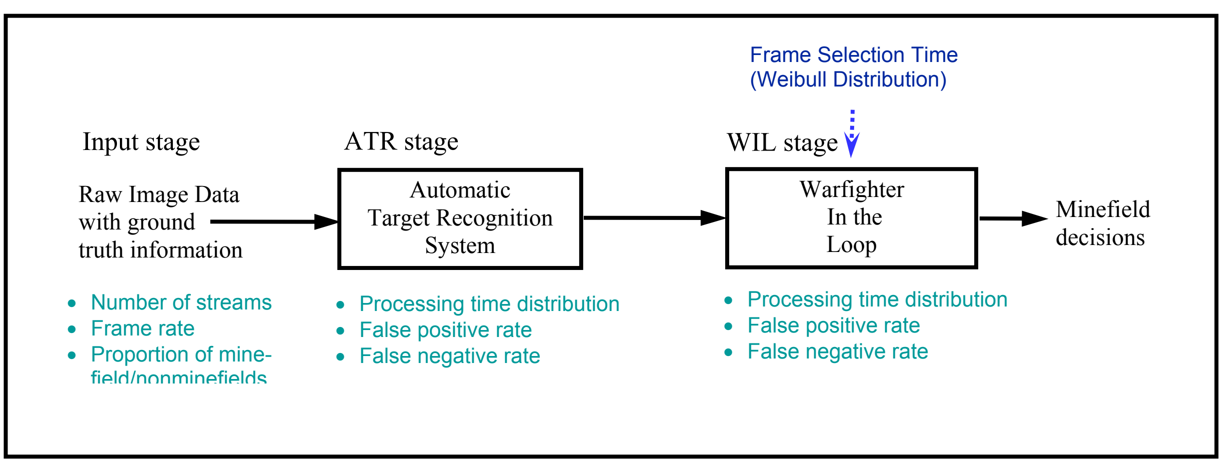

Figure 4: Simulation Framework with Controllable Parameters

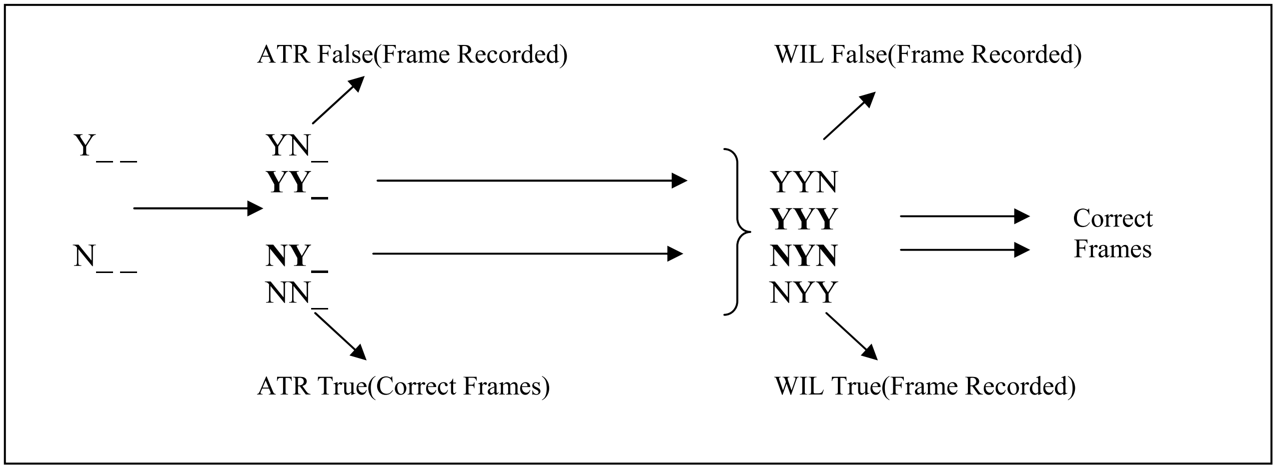

Figure 5: Frame Flagging at Each Stage

4.1.3 WIL Stage

The three controllable factors are: the WIL processing time, WIL probability of detection, and the WIL false alarm rate. The warfighter is presented with those segments which were tagged as mined by the ATR. This includes minefield segments and false alarms (Figure 5).

The time analysis which is covered in Section 2.2.3 shows how much time the user takes to analyze segments with no mines and those with mines. This has been used to determine the distribution of the processing time, which is modeled as Weibull distributions as discussed in Section 2.2.3. The other factors evaluated at the WIL stage, the probability of detection, and probability of false alarms, represents the effectiveness of individual warfighter in correctly detecting minefields or wrongly identifying non-minefields as minefields.

4.2 Frame Flagging at Each Stage

The variables can be defined as shown in the Figure 6.

a b c

Frame Definition(a, b, c)
a – Ground truth; binary(Y/N)
b – Decision by ATR; binary(Y/N)
c – Decision by warfighter; binary(Y/N)
A “Y” indicates a minefield while “N” indicates a non-minefield at corresponding stage.

Figure 6: Frame Definition for Flagging the Frames.

Ground truth is the a prior known correct information whether the segment is minefield or not. In real analysis, we do not have this information. But for our analysis, we have to assign different probabilities of selection for both minefield and non-minefield segments. So ‘a’ can be Y or N depending on whether the frame is minefield or non-minefield respectively. These two are separately analyzed at the ATR stage.

The decision at the ATR is ‘b’ which can also be a Y or N depending on the accuracy of the ATR in selecting the segment as minefield or non minefield. If ATR flags a minefield segment as a non minefield segment (YN) it would not be passed into the next stage. This is an error, so this is one factor which has to be considered for analysis. If the minefield segment is correctly flagged it is marked (YY) and is passed to the WIL stage. If a non minefield segment is correctly flagged (NN), it is rejected because we do not need correctly detected non-minefield segments to be passed to the WIL. But if it is wrongly flagged as a minefield segment (NY), it is passed onto the warfighter for further analysis. This condition is a false alarm by the ATR, but since it is detected as a minefield it has to be passed to the WIL stage.

The segments arriving at the warfighter are: correctly flagged minefields (YY), and wrongly flagged non-minefields (NY). There are four different possibilities at this stage. The warfighter can correctly flag the minefield segments (YYY) or he/she can make an error by choosing a minefield to be a non minefield (YYN). Since the latter is an error it is recorded for analysis. Similarly, if the warfighter flags the non-minefield wrongly (NYY) this segment is recorded since it is an error. The correctly flagged non-minefield segments are (NYN).

Therefore we have three error values that are recorded for analysis, the wrongly flagged ATR minefield segments (YN), wrongly flagged WIL minefield segments (YYN), and wrongly flagged WIL non minefield segments (NYY).

5 DESIGN OF EXPERIMENTS

A simulation model in Arena® of Rockwell Automation (Kelton, Sadowski, and Sturrock 2003) was created to study the performance of the modeled system.

5.1 Controllable Factors and Levels Considered

Section 3.1 discusses several factors that are considered. The simulation parameters that were used in each section is explained in detail in the following subsections.

5.1.1 Input Stage

The frame arrival rate and also the proportion of the minefield/no-minefield segments are the two parameters which were considered for the actual simulation. Multiple streams were not considered since it was beyond the scope of this paper. Table 1. shows the factors chosen:

Table 1: Parameters at Input Stage.

Frame rate	1/3Hz			
Probability of Mine segments	0.005	0.010	0.020	0.050

Each segment from a single UAV was passed to an ATR at a constant rate of one segment per 3sec which is 1200 segments/hr. For analysis, we are assuming that there is no overlapping of segments. A number of segments were passed for the total simulation with multiple replications.

The other parameter which is considered is the proportion of the minefield/non-minefield segments passed into the ATR. We have no information of the actual percentage of minefield/non-minefield segments coming from a UAV. But we know that only very small percentage of segments will have mines in a large area covered by the UAV. Four levels were considered here, 5% of minefield segments which means 20 minefield segments per hour, 2% which is 8 minefield segments/hr, 1% which is 4 minefield segments/hr and 0.5% which is 2 minefield segments/hr.

5.1.2 ATR Stage

Three parameters are considered in this stage. They are the processing time at the ATR, percentage of minefield segments passed, and percentage of non-minefield segments passed. The parameters and levels are shown in Table 2. In the simulation, ATR processing time is sub-divided into 3 levels. A constant value of 3 sec processing time was used to analyze the actual wait time at the warfighter stage irrespective of the queue caused at the ATR stage. Since the frame is also arriving at a constant rate of 3 sec, no queue is formed at the ATR stage. The second distribution used was a uniform distribution with a maximum value of 4 and a minimum value of 2. This distribution would better approximate the behavior of the ATR as the processing time.

Table 2: Parameters at the ATR Stage

ATR processing time	Constant (3)	Uniform (2,4)	Poisson (3)
PD @ ATR	0.95		
PFA @ ATR	0.005	0.015	0.025

The third distribution used was a Poisson distribution with a mean value of 3. This was also done to study the queue formed at the WIL with the influence of the ATR. The second parameter considered was the percentage of minefield segments passed by the ATR. The objective requirement for probability of detection at ATR is 0.95. The rest 5% minefield segments are rejected as missed detections. This factor is kept fixed with single level.

The third parameter is the percentage of non-minefield segments which are passed by the ATR. The objective requirement calls for 0.5 false alarms per km^2 which would correspond to a probability of false alarms at approximately 0.5%. For analysis we are considering 3 levels of selection rates. The probabilities chosen are 0.005, 0.015, and 0.025 of non-minefields being passed as minefield segments. These segments are actual false alarms detected by the ATR.

5.1.3 WIL Stage

At the WIL stage, three parameters are considered as in the case of ATR stage. They are: processing time at WIL, percentage of minefields passed, and percentage of non-minefields passed. This is illustrated in Table 3.

As discussed in Section 2.3.4, minefields and non-minefields are analyzed separately with two different Weibull distributions. The analysis done in Section 2.3.4 considers only an area of 50x20m, but the actual area would be 120x60m. Hence it is assumed that the user takes more time in deciding on the actual area. In order to account for this mismatch between the prior experimental and the proposed operational environment, the scale parameter, and delay of the modeled Weibull distribution are magnified with a factor of 2 and 4 as shown in Table 3. These two levels of factors are called Fac 2 and Fac 4 levels.

Table 3: Parameters at the WIL

Detection Time (Weibull Distribution)		Minefield		Non-Minefield	
		Fac 2	Fac 4	Fac 2	Fac 4
	Scale	55.28	110.55	32.58	65.16
	Shape	1.38	1.38	0.99	0.99
	Delay	10.00	20.00	6.00	12.00
PD@WIL	0.95				
FPA@WIL	0.20				

The second parameter is the probability of detection of WIL. The objective requirement at WIL stage requires a probability of detection of 95%. Laboratory experiments with test images show a 100% probability of detection for minefield by human operator (Reddy, Agarwal, Hall, Brown, and Woodard 2005). For this reason only one level is considered here at a PD of 0.95.

Similarly, for the third parameter, the objective requirements for WIL is to reduce the false alarms by a factor of 5, which means that only one in every five ATR false alarm segments is called a false alarm by WIL, which gives a probability of false alarm at WIL at 0.2. Here again we consider only one level for analysis.

5.2 Trials

As discussed above the number of parameters and levels that were used are summarized in Table 4.

Table 4: Calculation of Number of Replications for Simulation

Parameter	Levels	DOF
Frame rate	1	
Proportion of Minefield segments	4	3
ATR processing time	3	2
Probability of false detection at ATR	3	2
Probability of detection at ATR	1	
Detection Time for WIL	2	1
Probability of false detection at WIL	1	
Probability of detection at WIL	1	
Total Trials & Replications	72	12

The number of replications is determined by the degree of freedom (DOF) from the levels of each parameter as shown in Table 4. The factorial of the degrees of freedom of the parameters gives the total number of replications. So 72 trials were run with 12 replications to obtain reasonable results. The replication length was chosen to be 28800 which represents 8 hours worth of data.

6 OBSERVATIONS

A chi-square test indicated that that using different distributions (Constant, Uniform, and Poisson) for modeling the processing time at ATR stage did not have any significant influence on the waiting time for segments in the queue at the human stage. This is expected since the average ATR processing time in each of the three levels considered is 3 seconds which is same as the segment arrival time. For this reason this factor is not discussed further in the paper..

The error count for segments at three different stages is calculated. The wrongly detected minefield segments at the ATR stage, wrongly detected minefield segments at the WIL stage, and wrongly detected no-minefield segments at the WIL stage. The count values were noted for each of 72 runs. Some of the runs are listed in the Table 5. Value of different levels, average waiting time, and average frame waiting at WIL stage are also shown. Table 5 also shows the parameters and the corresponding error counts at the ATR and WIL stage. The expected value of the error count can be calculated using the corresponding equations. The expected number of minefield segments which was wrongly detected by the ATR is represented by :

$$YN_{ATR} = X \cdot P_{MF} \cdot (1 - P_{MDATR}) \tag{3}$$

where,

- YN_{ATR} is the expected number of wrongly detected ATR segments.
- X is the number of segments passed.
- P_{MF} is the probability of minefield segments
- P_{MDATR} is the probability of detection of minefield segments at ATR.

The expected value of minefield segments rejected by WIL can be represented by:

$$YYN_{WIL} = X \cdot P_{MF} \cdot P_{MDATR} \cdot (1 - P_{MDWIL}) \tag{4}$$

where,

- YYN_{WIL} is the expected number wrongly detected minefield segments.
- P_{MDWIL} is the probability of detection of minefield segments at WIL

And finally the expected value of the non minefield segments which are wrongly selected by the human can be represented by:

$$NYY_{WIL} = X \cdot (1 - P_{MF}) \cdot (1 - P_{NMDATR}) \cdot (1 - P_{NMDWIL}) \tag{5}$$

where,

- NYY_{WIL} is the expected number of wrongly detected non-minefield segments(false alarms).
- P_{NMDATR} is the probability of detection of non-minefield segments at ATR.
- P_{NMDWIL} is the probability of correct detection of non-minefield segments at WIL.

From the above equations and the trials, the expected values of the counter was calculated and is shown in Table 6. X is taken to be 9200 segments for every replication. P_{NMDWIL} is taken as 0.80, P_{MDATR} is taken as 0.95, and P_{MDWIL} is taken as 0.95 in every case as discussed in Section 4.1.3. The expected and observed counter numbers were determined for each treatment. This was plotted against the runs in Figures 7-9. Figure 7 shows the counter value variation at the ATR stage where minefields are rejected by the ATR. The blue line shows the expected counter values at each runs and the red line shows the observed counter values. Deviations from the expected value were calculated statistically and the mean value of the deviation of the total number of counters was found to be only 0.13, which is an acceptable range. Figures 7-9 also

Table 5: Error Counts at Certain Runs in the Simulation; Poisson Distribution was Chosen as ATR Processing Time

Prop of MF	PD NM ATR	Time Factor WIL	Counter YN_{ATR}	Counter YYN_{WIL}	Counter NYY_{WIL}	Counter total	Wait Time WIL	Number Waiting WIL
0.05	0.995	2	21.17	22.08	9.33	52.58	827.94	14.40
0.05	0.995	4	23.00	9.83	4.33	37.17	7561.38	128.99
0.05	0.975	2	22.17	17.83	33.75	73.75	3064.52	73.10
0.05	0.975	4	24.57	9.42	16.92	50.83	9087.52	212.56
0.01	0.995	2	4.42	4.33	10.25	19.00	13.20	0.06
0.01	0.995	4	5.00	3.17	9.58	17.75	66.86	0.33
0.01	0.985	2	3.75	4.25	47.58	55.58	39.22	0.46
0.01	0.985	4	5.25	4.08	43.67	53.00	1426.04	16.46
0.005	0.995	2	2.33	2.42	8.92	13.67	8.15	0.03
0.005	0.995	4	1.42	1.92	10.25	13.58	32.17	0.10
0.005	0.985	2	2.25	2.92	47.50	52.67	25.19	0.25
0.005	0.985	4	2.33	2.67	46.08	51.08	234.11	2.32

Table 6: Expected Error(Counter) Values at Different Stages

P_{MF}	P_{NMDATR}	YN_{ATR}	YYN_{WIL}	NYY_{WIL}
0.05	0.995	23.00	21.85	8.74
0.05	0.975			43.70
0.01	0.995	4.60	4.37	9.11
0.01	0.975			45.54
0.005	0.995	2.30	2.19	9.15
0.005	0.975			45.77

shows us that the deviations are in the acceptable range. A higher difference is observed in the case of the high probabilities of minefields, and high false alarm rate by ATR since there is a significant waiting time at WIL stage which reduces the throughput. Hence deviation is higher for the case of WIL processing time corresponding to factor 4.

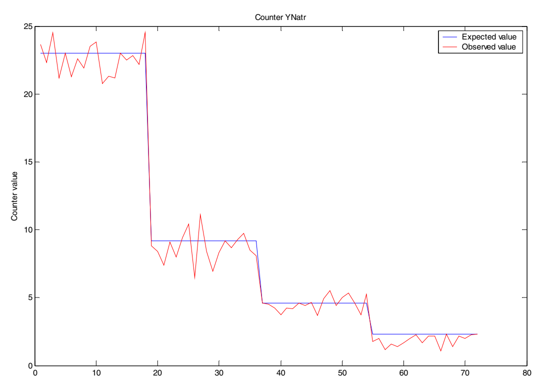

Figure 7: YN_{ATR} Counter Value Deviations

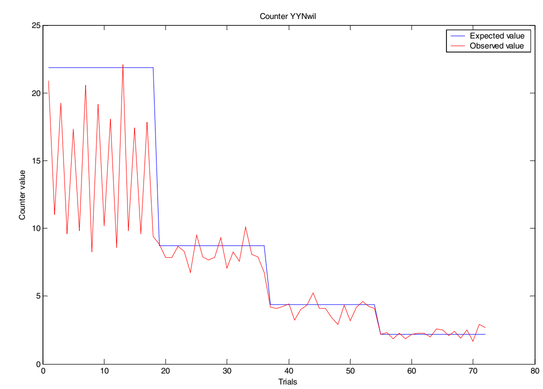

Figure 8: YYN_{WIL} Counter Value Deviations

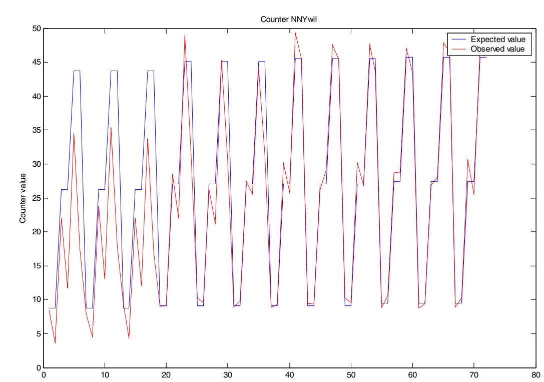

Figure 9: NNY_{WIL} Counter Value Deviations

Since the WIL waiting time was statistically independent of the ATR processing time, a better estimate of the parameters at the WIL stage can be obtained by averaging the time values of all the three distributions. Figures

10-13 shows the average waiting time and number of segments in the queue in a color scale, blue color being the minimum waiting time and the red color being the maximum waiting time. The value of average waiting time and number of frame waiting is plotted in logarithmic scale and is represented using the color bar by the side of the plot. The Figures 10-11 shows the value of average time when there is x% of minefields in ground-truth and there is y% of false alarm for non-minefield segments at ATR. In Figure 10-11, WIL decision time corresponds to factor 2 and factor 4 respectively. Similarly Figure 12-13 shows the results for number of segments waiting at WIL stage. Here also, Figure 12-13 show waiting times corresponding to time factor 2 and factor 4 respectively.

Figure 10: Color Map of Average Waiting Time at Warfighter with a Time Factor of 2.

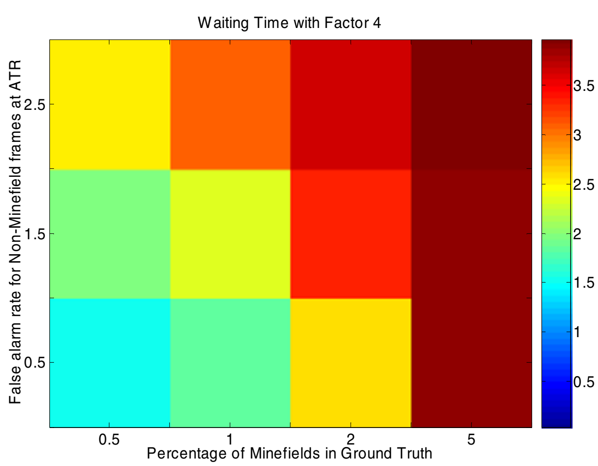

Figure 11: Color Map of Average Waiting Time at Warfighter with a Time Factor of 4.

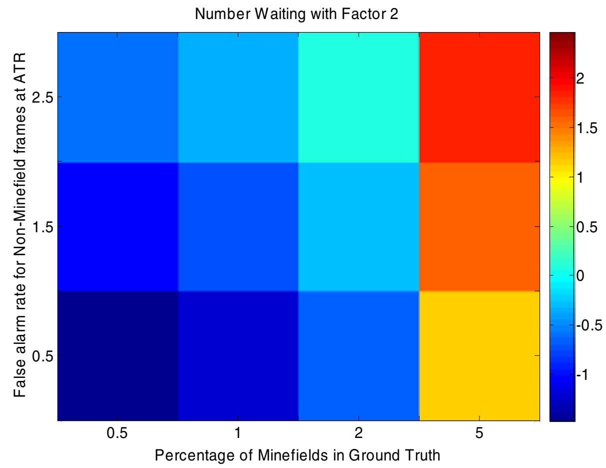

Figure 12: Color Map of Average Number of Segments Waiting at Warfighter with a Time Factor of 2.

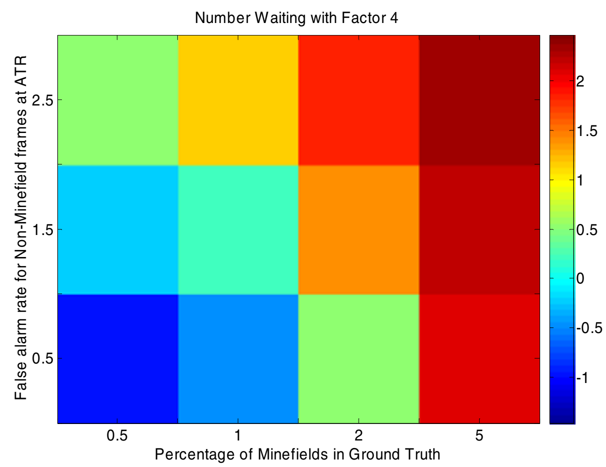

Figure 13: Color Map of Average Number of Segments Waiting at Warfighter with a Time Factor of 4.

Based on Figures 10-13 several inferences can be made on the selection of appropriate parameters at different stages of the model. The best case can be identified as the lower left corner in the plot where the waiting time and number of segments in queue is small (<100seconds and <1 frame).

In this case, we have only 0.5% of minefield segments in the whole set of ground truth which corresponds to about 6 minefield segments/hr of which 95% are passed to the warfighter. Also only 0.5% of non-minefields are passed to WIL representing 6 segments per hour. Thus the user needs to process only 12 segments per hour and thus has sufficient time to process. This total is the least number of segments that could come to the warfighter in a run. Similarly the worst case scenario would be when we have 5% of minefield segments which is 60 minefield segments/hr and 2.5% of the non-minefield segments which is approximately 30 non-minefield segments/hr. This is too many for the warfighter to keep up with the frame rate. So the effective load on him increases and number of segments waiting at the queue at WIL will be larger(>200) as observed in Figure 13. Since there are more minefield segments in this case, there will be more detections at the ATR and the human will have to analyze more minefield segments which is more time consuming than non-minefield segments. Based on these results, in the case of single UAV, we can observe that acceptable waiting times are observed when the percentage of minefield segments in ground-truth is less than 1% and also when the false alarm rate for non-minefield segments is less than 1.5%. We can also see from Figure 12 and Figure 13 that the warfighter will be unable to handle the number of segments arriving when values are beyond the above mentioned limits resulting in a long queue and long waiting time.

7 CONCLUSION

Airborne minefield detection model was studied using a simulation model to evaluate the performance of a warfighter in the loop. Weibull distribution was considered with appropriate scale, shape, and offset values for minefield segments and non minefield segments was determined for this model. After the parameters were determined, a simulation study was performed. From the results, the effects of other blocks over the WIL were analyzed, and shown. It was observed that with the model, time characteristics of the warfighter could be effectively studied. It was found that the warfighters would not be able to handle the number of segments to process effectively when the percentage of minefield segments in ground truth is more than 1% and when the false alarm rate for non-minefield segments is more than 1.5%. This has significant implications on how to specify these systems for implementation. Future studies will focus on the presence of multiple streams of data from different sources.

REFERENCES

S. Agarwal, M. Reddy, R. H. Hall, J. W. Brown, T. J. Woodard. 2005. Evaluating Operator Performance in Aided Airborne Target Detection, *Proceedings of Defense and Security Symposium 2005 (SPIE-DSS'05)*. 5974: 102-112.

S.L. Earp, T.J. Elkins, B.C. Conrath. 1995. Detection of Random Minefields in Clutter, *Proceedings of SPIE Detection Technologies for Mines and Mine like Targets*, 2496: 412-420

Holmes, Q. A., Schwartz, C. R., and Seldin, J. H. 1995. Adaptive Multi-Spectral CFAR Detection of Landmines, *Proceedings of SPIE Detection Technologies for Mines and Mine-like Targets,* 2496: 421-432

Kotz, S; Balakrishnan, N., and Johnson, N. L. 1994. *Continuous Univariate Distributions*, Volume 1, Second Edition., A Wiley-Interscience Publication.

Kelton D.W., Sadowski R.P., and Sturrock D. 2003. *Simulation with ARENA*, McGraw-Hill, Science/ Engineering/ Mathematics, Third Edition.

Menon D., Agarwal S., Ganju R., and Swonger C. W. 2004. False Alarm Mitigation and Feature Based Discrimination for Airborne Mine Detection, *Proceedings of SPIE Detection Technologies for Mines and Mine like Targets IX*. 5415: 1163-1173.

M. Reddy, S. Agarwal, R. H. Hall, J. W. Brown, T. J. Woodard. 2005. Warfighter in the Loop : Mental Models in Airborne Detection, *Proceedings of Defense and Security Symposium 2005 (SPIE-DSS'05)*. 5794: 1050-1059.

Reed I.S. and Yu. X. 1990. Adaptive Multi-Band CFAR Detection of an Optical Pattern with Unknown Spectral Distribution, *IEEE Transactions On Acoustics, Speech and Signal Processing*, Volume 38, No. 10.

Sriram P., Agarwal S., Mitchell O.R. 2002. Gray-scale Moment Invariants for Airborne Mine Detection, Discrimination, and False Alarm Mitigation, *Proceedings of SPIE Detection Technologies for Mines and Mine like Targets* VII, 4742: 974-985.

AUTHOR BIOGRAPHIES

ABHILASH RAJAGOPAL is a graduate student currently working as a graduate research assistant in the Department of Electrical and Computer Engineering at University of Missouri, Rolla. He has a B.E. (Electronics and Communication) from Bharathiyar University, India. His research interests are agent based architecture, image processing. He is a member of IEEE. His email address is arrh3@umr.edu.

SANJEEV AGARWAL is a research assistant professor of Electrical and Computer Engineering in the University of Missouri-Rolla. He has completed his PhD (1998) in Electrical and Computer Engineering from University of Missouri-Rolla and B.Tech. and M.Tech. (1993) degrees form Indian Institute of Technology, Bombay. Dr. Agarwal joined the department of Electrical and Computer Engineering at University of Missouri-Rolla in 1998. Dr. Agarwal's research interests include machine vision, intelligent computing, image processing, multi-sensor fusion, automatic detection theory, airborne terrain analysis and reconnaissance, and virtual and augmented reality. Dr. Agarwal is a member of IEEE & SPIE. His email address is sanjeev@umr.edu.

SREERAM RAMAKRISHNAN is an assistant professor of Engineering Management and Systems Engineering in the University of Missouri- Rolla. He has a Ph.D. in Industrial Engineering from Pennsylvania State University, a M.S. (Industrial Engineering) from Binghamton University, and a B.Tech. (Mechanical) degree from University of Kerala, India. His research interests include distributed systems modeling, simulation-based control, and modeling control systems. He is a member of IIE and ASEE. His e-mail address is sreeram@umr.edu.